Human Apolipoprotein H May Have Various Orientations When Attached to Lipid Layer

Fu Wang, Xiao-Feng Xia, and Sen-fang Sui
Department of Biological Sciences and Biotechnology, State-Key Laboratory of Biomembrane, Tsinghua University, Beijing 100084, People's Republic of China

ABSTRACT Apolipoprotein H (ApoH), also known as β_2-glycoprotein I, is a plasma glycoprotein with its in vivo physiological and pathogenic roles being closely related to its interaction with negatively charged membranes. Although the three-dimensional crystal structure of ApoH has been recently solved, direct evidence about the spatial state of ApoH on the membrane is still lacking. In this work, the interactions of ApoH with the lipid layer are studied by a combination of lipid monolayer approach and surface concentration determination. The spatial state of the orientation of ApoH on the lipid layer is investigated by analyzing the process of membrane-attached ApoH molecules being extruded out from the phospholipid monolayer by compression. The results show that on neutral lipid layer ApoH has an upright orientation, which is not sensitive to the phase state of the lipid layer. However, on acidic lipid layer, ApoH may have two forms of orientation. One is an upright orientation in the liquid phase region, and the other is flat orientation on the condensed domain region. The variation of the spatial state of ApoH on the lipid layer may relate to a variety of its physiological functions.

INTRODUCTION

Apolipoprotein H (ApoH), also known as β_2-glycoprotein I, is a plasma glycoprotein either circulating as a free protein or associated to lipoproteins. This protein was found in human serum and described for the first time in 1961 by Schultze et al. (1961). ApoH is a 54-kDa single-chain glycoprotein consisting of five carbohydrate chains and 326 amino acid residues that can be divided into five short consensus repeat domains (Ichinose et al., 1990). ApoH has been chiefly focused on as the cofactor or autoantigen in antiphospholipid syndrome (APS), which is related to venous and arterial thrombosis, fetal loss, and thrombocytopenia (Blank et al., 1994; Shiozaka et al., 1994). Reports show that ApoH may have an important function in blood coagulation and clearance of apoptotic bodies from the circulation (Brighton et al., 1996). Some works indicate that the binding of ApoH with target membranes containing anionic phospholipids could induce agglutination and precipitation (Schousboe, 1979; Wurm, 1984). The interactions of ApoH with phospholipids are considered crucial in explaining its physiological or clinical roles. Many experiments have demonstrated that ApoH prefers to interact with anionic phospholipids (Wurm, 1984; Kertesz et al., 1995; Hagihara et al., 1995; Willems et al., 1996; Wang et al., 1998). Although it has been proved that both domains I and V exhibit lipid-binding properties, the fifth domain is especially important for phospholipid binding (Hagihara et al., 1995, 1997; Hunt and Krilis, 1994; Mehdi et al., 2000). The solution of the ApoH's crystal structure revealed four complement control protein modules. Also, a distinctly folding fifth C-terminal domain arranged to form an elongated fishhook-like molecule (Bouma et al., 1999; Schwarzenbacher et al., 1999). According to the three-dimensional structure it was supposed that a region that carries a large patch of positively charged residues in the fifth domain would provide electrostatic interactions with anionic phospholipid headgroups and an exposed membrane-insertion loop would yield specificity for the lipid layers.

The authors' previous work demonstrated that ApoH is an amphiphilic protein tending to insert into the negatively charged lipid monolayer. The previous work also showed that a conformational change of ApoH was induced when interacting with anionic phospholipid-containing vesicles (Wang et al., 1998, 1999, 2000). Both electrostatic and hydrophobic forces involved in the ApoH/membrane interactions were noticed in these studies. In the present work, the interaction of ApoH with the phospholipid monolayer was studied by using film balance and fluorescence techniques. The surface protein concentration was determined by the monolayer collection method. The spatial state of the orientation of ApoH on the lipid layer was investigated by analyzing the process of membrane-attached ApoH molecules being extruded out from the phospholipid monolayer by compression.

MATERIALS AND METHODS

Materials

Dimyristoylphosphatidylcholine (DMPC), dipalmitoylphosphatidylcholine (DPPC), distearoylphosphatidylcholine (DSPC), dipalmitoylphosphatidylglycerol (DPPG), and FITC isomer I were purchased from Sigma Chemical Co (St. Louis, MO). The fluorescent lipid probe (rhodamine-dioleoylphosphatidylethanolamine (DOPE)) was purchased from Avanti Polar Lipids (Alabaster, AL). Heparin-Sepharose CL-6B was purchased from Pharmacia (Uppsala, Sweden). The deionized water was obtained from the Microelectronic Institute of Tsinghua University with resistivity more than

Submitted December 3, 2001, and accepted for publication April 8, 2002.
Address reprint requests to Dr. Sen-fang Sui, Department of Biological Sciences and Biotechnology, Tsinghua University, Beijing 100084, People's Republic of China. Tel.: 8610-62784768; Fax: 8610-62784768; E-mail: suisf@mail.tsinghua.edu.cn.

0006-3495/02/08/985/09 $2.00

18 MΩm. All the other chemicals used were of analytical grade and manufactured in China. Unless stated otherwise, all subphase buffers for the monolayer were 25 mM, pH 7.4 Tris/HCl.

Preparation of ApoH

ApoH was purified from human serum, as described by Wang et al. (1999). Briefly, 2.5 ml of perchloric acid (70%, v/v) was gradually added to 100 ml of fresh human serum at 4°C. After stirring for 15 min, the sample was centrifuged at 13,000 rpm for 20 min. The supernatant was neutralized to pH 8.0 by adding saturated Na_2CO_3 solution. It was then dialyzed against a NaCl, Tris/HCl buffer (0.02 M Tris-Cl, 0.03 M NaCl, pH 8.0) for more than 36 h. The dialysate was applied to the heparin-Sepharose CL-6B column that had been equilibrated with the same buffer. The adsorbed proteins were eluted stepwise, using 0.02 M Tris/HCl buffer (pH 8.0), with an increasing molarity of NaCl. The fraction eluting in a linear NaCl gradient from 0.15 to 0.60 M was collected. Checked with SDS-PAGE, the protein sample showed one protein band at an apparent molecular mass of 54 kDa after silver staining. After dialysis against bi-distilled water, the purified ApoH was lyophilized and stored at −70°C. Protein concentration was determined by absorption spectroscopy (ϵ_{280} = 0.9 ml/(mg·cm)).

Conjugation of ApoH with FITC followed the method described by Mi et al. (1997), with some modifications. Briefly, 20 nmol of ApoH with 160 nmol of FITC were dissolved in 1 ml of a $NaHCO_3/Na_2CO_3$ (pH 9.0) buffer. The mixture was then adequately homogenized and incubated for 24 h at 4°C. Unreacted reagent was removed by overnight dialysis against 25 mM, pH 7.4, Tris/HCl. The labeled ApoH was further purified by G-25 gel filtration chromatography in the same buffer. The FITC/ApoH ratio was estimated to be 3:1 from the absorbance at 495 nm and 280 nm.

Formation of monolayer

Monolayer experiments to measure pressure-area (π-A) isotherms were carried out in the Teflon trough (320 mm × 75 mm × 7 mm, with total subphase volume of 168 ml) of a KSV5000 Langmuir film balance system. Phospholipids were dissolved in chloroform/methanol (3:1 v/v) to get a concentration of 1 mg/ml. Droplets of lipid solutions were spread on the subphase (with or without ApoH) using a microsyringe. The initial surface pressure was designated to be 0.1 mN/m. After incubation for 10 h at a temperature of 21 ± 0.5°C to make proteins adequately penetrate into the monolayer, the lipid film was then compressed at a speed of 1 Å^2 molecule^{-1} min^{-1}.

Microfluorescence film balance

The microfluorescence film balance system was constructed using a Nikon Diaphot-TMD inverted epifluorescence microscope and a computer-controlled film balance. The microscope was equipped to accommodate for an extremely long-working-distance objective. A rectangular Teflon trough with dimensions of 20 cm × 8 cm × 0.8 cm was fixed onto the movable stage of the microscope. A 40-mm-diameter glass window was located at the bottom of the trough above the microscopic objective. Temperature was controlled by water circulation in the base of the trough. The excitation of the fluorescent lipid probe in the monolayer was performed by illumination with a 100-W high-voltage mercury lamp. Several filter combinations for different wavelength ranges were available. Pictures were taken with a low-light-level SIT camera (Hamamatsu c2400) and recorded with a VHS video recorder (Panasonic HD-100).

Surface protein concentration determined by the monolayer collection method

Different assays of surface collection have been introduced (Gargouri et al., 1986, 1989; Aoubala et al., 1995; Rietsch et al., 1977; Momsen and Brockman, 1997). Rietsch et al. (1977) developed a collection system based on surface aspiration. The adsorption of surface phase to a hydrophobic support was introduced by Momsen and Brockman (1997). For these collection methods the protein concentration was determined by radioactivity counting. In this work, a new method has been developed to determine protein concentration at the air/water interface, which is based upon monolayer aspiration and fluorescence measurement. The procedure is briefly described as follows.

At first, a plot exhibiting a relationship between fluorescence emission intensity (θ) and protein concentration (c) was carefully measured, using a fluorescence spectrometer for calibration. The function between c and θ exhibited a straight line (data not shown), indicating a linear correlation between them in the protein concentration region used in the current measurements. This can be expressed as the following formula:

$$\theta = kc \tag{1}$$

The monolayer collection was performed as follows. A monolayer was formed at the air/water interface by spreading phospholipid onto a subphase that contained desired bulk concentration of FITC-labeled ApoH, for example, 3 nM and 5 nM in the current case. The initial surface pressure 0.1 mN/m was controlled. After incubating for 10 h (at a temperature of 21 ± 0.5°C) to make the proteins thoroughly interact with the monolayer-containing interface, a mixed monolayer (a monolayer of spread lipid mixed with penetrated protein) was formed. The mixed monolayer was then slowly compressed by moving the barrier (at a speed of 1 Å^2 molecule^{-1} min^{-1}) to a desired surface pressure (π_0) with a surface area of A_0. Before performing monolayer collection, Γ was defined as the surface protein density and c_b as the bulk protein concentration. Here, c_b is corresponding to the fluorescence emission intensity θ_b. Then, a part of the mixed monolayer together with a small amount of monolayer-adsorbed subphase solution was carefully collected by vacuum aspiration. The collected solution was then directed into a glass apparatus. The volume of the collected solution was v_c, and the protein concentration in v_c was c_c (with corresponding fluorescence emission intensity θ_c). The reduced surface area A_r, i.e., the surface area change after monolayer collection, can be determined by moving the barrier to the position at which the surface pressure reaches the original π_0.

The proteins in the collected solution can be divided into two parts according to where they came from: the interface and the adsorbed bulk solution. Thus:

$$v_c c_c = \Gamma A_r + v_c c_b \tag{2}$$

Here, it is assumed that the monolayer is an ideal geometrical plane, and only a single layer of protein adsorbs at the interface. Hence:

$$\Gamma = \frac{1}{A_r}(v_c c_c - v_c c_b) = \frac{v_c}{A_r}(c_c - c_b) = \frac{v_c}{A_r k}(\theta_c - \theta_b) \tag{3}$$

All parameters on the right side of the formula (Eq. 3) can be determined by measurements. Thus, the surface concentration of protein can be calculated. The advantage of this measurement method is that the influence of protein adsorption onto the sides of the trough, which is always interfering in calculation, can be totally eliminated.

The fluorescence intensity of the surface-collected solution was measured with a Hitachi M850 fluorescence spectrophotometer in a darkroom at 21°C. The excitation was at 495 nm and the emission at 520 nm. The emission and excitation slit widths were set at 5 nm. Before measuring fluorescence the collected solution was thoroughly mixed using an ultrasonic homogenizer.

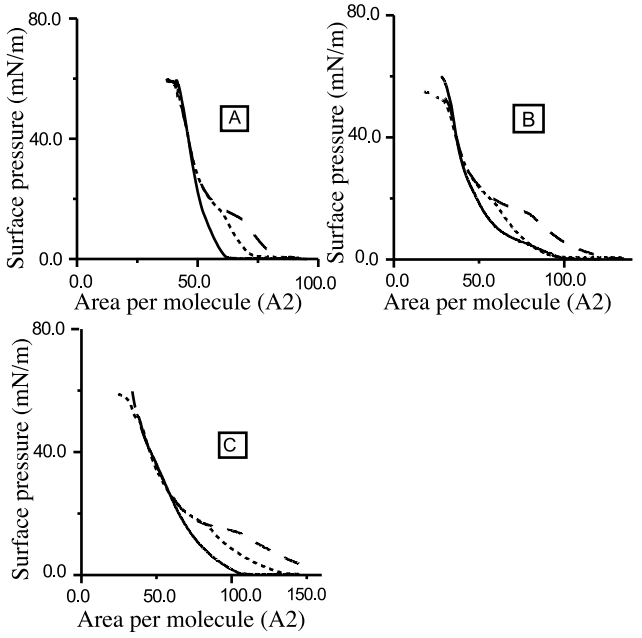

FIGURE 1 π-A isotherms of neutral phospholipid monolayers on solution with or without ApoH. Solid lines show the isotherms of pure DSPC, DPPC, and DMPC monolayer, respectively; dotted and dashed lines are isotherms of 20 nmol of neutral phospholipid on a subphase buffer with 3 nM or 5 nM ApoH. Subphase buffer is 25 mM Tris/HCl, pH 7.4. Temperature is 21 ± 0.5°C.

RESULTS

Interaction of ApoH with neutral phospholipid monolayers

The interaction of ApoH with monolayers of DSPC, DPPC, and DMPC was studied by film balance and with a fluorescence microscope. In Fig. 1, the isotherms of different neutral phospholipids on the pure buffer and 3 nM and 5 nM ApoH solutions are compared. Fig. 1 *A* shows that the three isotherms of DSPC on the pure buffer (solid line) and on both ApoH solutions (dotted and dashed lines) exhibit a similar compressibility $[-(1/A)(\partial A/\partial \pi)]$ in the lower surface pressure region. With increasing surface pressure the two isotherms of DSPC on ApoH solution approach an inflection. Over the inflections the two isotherms gradually come together at a pressure of ~18.0 mN/m. After this the two isotherms have exactly the same π-A trace. This indicates that the two mixed monolayers (dotted and dashed lines) have the same composition in this pressure region. Next, these two isotherms approach the pure DSPC monolayer. Finally, the three isotherms overlap each other when the surface pressure is ~35.0 mN/m. Having the same π-A trace indicates that the three monolayers now have the same composition, suggesting that compression has completely extruded out the incorporated ApoH molecules.

The similar phenomena were also found from Fig. 1, *B* and *C*. The only discrepancy is the isotherm of pure DPPC monolayer in the low-surface-pressure region (solid line in Fig. 1 *B*). This is because the pure DPPC monolayer exhibits phase transition at the surface pressure π_m of ~6.0mN/m. Such phase transition is depressed after ApoH incorporation as indicated by the dotted and dashed lines shown at the corresponding pressure.

The surface concentration of ApoH was measured and calculated in terms of the monolayer collection method mentioned above. The experimental values in Eqs. 2 and 3 are shown in Table 1. Table 1 represents surface concentration of ApoH in a mixed monolayer under different surface pressures. The calculated parameters of an ApoH-DPPC mixed monolayer at different surface pressures are shown in Table 2. It can be seen in the lower pressure region, i.e., the pressure below 18.0 mN/m (18.0 mN/m corresponds to the inflection of the dotted line in Fig. 1 *B*), that the average surface density of ApoH increases (the average area per ApoH decreases), while the total number of proteins remain nearly constant. This indicates that during the compression in the lower-pressure region, ApoH molecules can be condensed without leaving the interface. When surface pressure is above 18.0 mN/m, the total number of proteins decreases with increasing surface pressure, indicating that a certain amount of proteins are extruded out. It can be estimated that about one fourth of the original mem-

TABLE 1 Measurement of surface concentration of ApoH at the DPPC monolayer

Surface pressure π (mN/m)	Bulk protein concentration C_b (μg/ml)	Collected protein concentration C_c (μg/ml)	Collected solution volume v_c (ml)	Collected surface area A_r (mm^2)	Surface ApoH concentration Γ (ng/mm^2)*	Average surface ApoH concentration Γ_a (ng/mm^2)†
9.8	0.16	3.12	3.0	3810	2.33	2.39 ± 0.14
12.3	0.16	1.52	3.4	1740	2.66	2.63 ± 0.16
16.0	0.15	2.09	4.0	2775	2.80	2.76 ± 0.17
18.0	0.16	2.71	4.6	4020	2.92	2.89 ± 0.17
22.0	0.17	1.28	7.9	3315	2.65	2.78 ± 0.17
26.0	0.17	1.73	4.5	2445	2.87	2.89 ± 0.17
30.0	0.18	1.14	6.9	2250	2.94	3.01 ± 0.18

*$\Gamma = \frac{v_c}{A_r}(c_c - c_b)$.

†Γ_a is the average value of surface concentration of ApoH obtained from three independent measurements.

TABLE 2 Parameters of the mixed monolayer of DPPC and ApoH at different surface pressure

Surface pressure π (mN/m)	Total area of mixed monolayer S (cm^2)*	Extended area after ApoH penetration A_{ex} (cm^2)	Average area per ApoH A_a (Å^2)†	Total number of ApoH N_t ($\times 10^{14}$)‡	Degree of condensation ϕ§
9.8	105.83	13.34	3470 ± 208	3.05	0.28 ± 0.05
12.3	100.52	14.90	3161 ± 190	3.18	0.33 ± 0.05
16.0	93.77	15.09	3005 ± 180	3.12	0.39 ± 0.05
18.0	89.57	13.94	2878 ± 173	3.11	0.45 ± 0.05
22.0	79.09	8.94	2989 ± 179	2.65	0.62 ± 0.05
26.0	70.20	6.30	2873 ± 172	2.44	0.71 ± 0.05
30.0	63.90	0.88	2763 ± 166	2.31	0.91 ± 0.05

*S and A_{ex} were measured from the π-A isotherms of Fig. 1 B.

†$A_a = \frac{M_w \times 10^{23}}{N_A} \times \frac{1}{\Gamma_a}$, where Γ_a is represented in Table 1, and N_A equals to 6.02×10^{23}.

‡$N_t = \frac{S}{A_a}$, where $M_w = 5.4 \times 10^4$ g/mol, which is the molecular weight of ApoH.

§ϕ was measured according to the fluorescence microscope images.

brane-attached ApoH were squeezed into subphase as the surface pressure increased from 18.0 to 30.0 mN/m.

Direct evidence for ApoH adsorption came from microfluorescence studies. In particular, the monolayer pressure was kept at a two-phase coexistence region. In the two-phase region the condensed phase exists as discrete domains within a continuous liquid phase. This phenomenon can be visualized using a fluorescent lipid probe that predominantly distributes in the liquid phase. The surface distribution of the FITC-labeled protein can also be directly observed. Fig. 2 represents a series of micrographs of DPPC monolayers with ApoH taken at the surface pressures in the two-phase coexistence region. In the first case, the images of Fig. 2, A and B were taken at the surface pressure 18.0 mN/m, which is around the inflection of the dotted line exhibited in Fig. 1 B. It can be seen that the light region in Fig. 2 B emitted from the distributed FITC-labeled ApoH has a similar contour to that of Fig. 2 A from the fluorescent lipid probe. This indicates that ApoH predominately penetrates into the monolayer region that is in the liquid phase. Such a phenomenon is understandable for general membrane proteins, as the high packing density in the condensed phase does not allow for distortion due to protein penetration (Möhwald, 1990; Liu et al., 1995; Mi et al., 1997). In the second case, the images of Fig. 2, C and D were taken at a higher pressure (~30.0 mN/m). Although the two-phase coexistence can still be observed, the contrast between dark and light regions in Fig. 2 D becomes weaker than that in Fig. 2 C. Because the pattern of the image in Fig. 2 D is due to the emission of FITC-labeled protein, a hazy contrast suggests that the FITC-labeled proteins are also present in the condensed phase region. Here, ϕ is defined as the degree of condensation, which is the ratio of dark area to total area in the lipid fluorescence images. The ϕ values of the DPPC monolayer at different surface pressures are listed in Table 2. The results demonstrate that ϕ increases with increasing surface pressure, indicating that DPPC monolayer becomes more condensed.

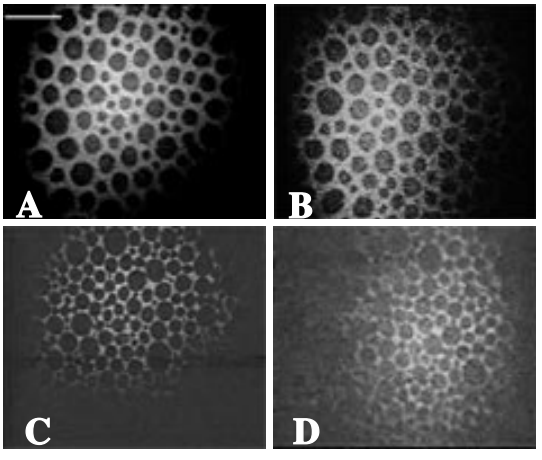

FIGURE 2 Fluorescence microscope images of the ApoH-DPPC mixed monolayer. (A and C) Images observed from the optical emission of fluorescent lipid probe; (B and D) Images observed from the optical emission of FITC-labeled ApoH. (A and B) Observed at a surface pressure of 18.0 mN/m; (C and D) 29.0 mN/m. Subphase buffer is 3 nM ApoH, 25 mM Tris/HCl, pH 7.4. Temperature is 21 ± 0.5°C. Scale bar (A), 50 μm.

Interaction of ApoH with anionic phospholipid monolayer

Interactions of ApoH with the DPPG monolayer were also studied by film balance and microfluorescence methods. The results are shown in Figs. 3 and 4. As shown in Fig. 3, the isotherms of DPPG on a pure buffer and 3 nM and 5 nM ApoH solutions are compared. They exhibit a similar compressibility in the lower-surface pressure region. This feature is identical with that observed in Fig. 1 for neutral PC monolayers. The results also show some other similar features. The inflection occurs in both isotherms of mixed monolayers (dotted and dashed lines). The two isotherms of mixed monolayers tend to overlap with the pure DPPG

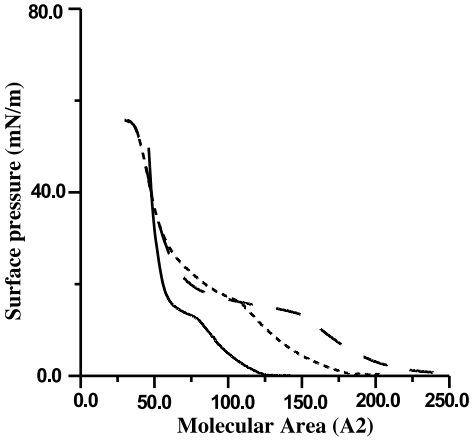

FIGURE 3 π-A isotherms of the DPPG monolayer on a buffer solution with and without ApoH. Solid line shows the isotherm of pure DPPG; dotted and dashed lines are those of 20 nmol DPPG on solution with 3 nM or 5 nM ApoH, respectively. Subphase buffer is 25 mM Tris/HCl, pH 7.4. Temperature is 21 ± 0.5°C.

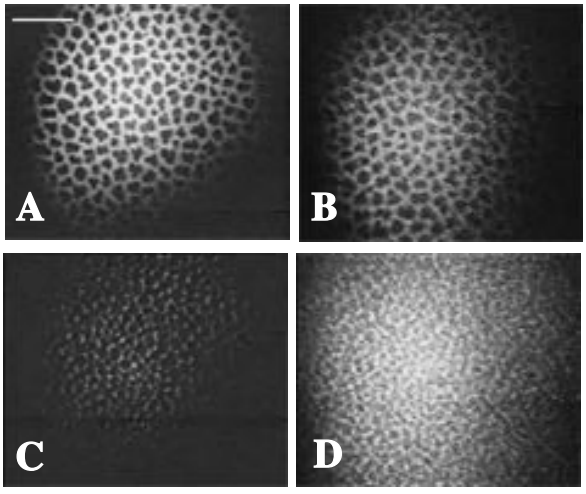

FIGURE 4 Fluorescence microscope images of the ApoH-DPPG mixed monolayer. (*A* and *C*) Images observed from the optical emission of the fluorescent lipid probe; (*B* and *D*) Images observed from the optical emission of FITC-labeled ApoH. (*A* and *B*) Observed at a surface pressure of 16.0 mN/m; (*C* and *D*) 32.0 mN/m. Subphase buffer is 3 nM ApoH, 25 mM Tris/HCl, pH 7.4. Temperature is 21 ± 0.5°C. Scale bar (*A*), 50 μm.

monolayer when surface pressure is high enough. Although similarities are apparent, there is also a difference. A discrepancy exists in these results when compared with Fig. 1. In particular, when surface pressure exceeds the inflection the dashed line exhibits a certain compression hysteresis before the two isotherms come to an identical trace. The phenomenon of compression hysteresis hints that electrostatic interaction between ApoH and DPPG may influence the protein behavior against compression.

Table 3 represents the experimental values of Eqs. 2 and 3 for the ApoH-DPPG mixed monolayer (subphase concentration of ApoH is 3 nM) under different surface pressures. The calculated parameters are shown in Table 4. When surface pressure increases above 16.0 mN/m (corresponding to the inflection of dotted line in Fig. 3), the total number of proteins decreases and the average surface density of ApoH also decreases. It can be estimated that about two-thirds of the original membrane-attached ApoH were squeezed into the subphase when the surface pressure increased from 16.0 to 32.0 mN/m. At the same time, the average surface density was decreased by about half. This phenomenon is different from that in the case of the DPPC-ApoH mixed monolayer. In the latter case, the surface density remains constant while the total number of proteins decreases when surface pressure increases above 18.0 mN/m.

Fig. 4 shows the fluorescence micrographs of pure DPPG and ApoH-DPPG mixed monolayers (DPPG on a pure buffer and on a solution of 3 nM ApoH, respectively) under different surface pressures. In the first case, the two images of Fig. 4, *A* and *B* were taken at a pressure of 16.0 mN/m. The two images show that, although ApoH prefers to be distributed in the liquid phase of the monolayer, the weakness in contrast between dark and light domains can be observed. This phenomenon becomes more obvious in the images of Fig. 4, *C* and *D*. In this case, the two images were taken at a relatively high pressure, 31.8 mN/m. From the image of Fig. 4 *D* it can be seen that the dark domains display more fluorescence, indicating that the protein molecules are also distributed on dark domains. The ϕ values of

TABLE 3 Measurement of the surface concentration of ApoH at the DPPG monolayer

Surface pressure π (mN/m)	Bulk protein concentration C_b (μg/ml)	Collected protein concentration C_c (μg/ml)	Collected solution volume v_c (ml)	Collected surface area A_r (mm^2)	Surface protein concentration Γ (ng/mm^2)*	Average surface ApoH concentration Γ_a (ng/mm^2)†
16.0	0.16	3.26	2.6	4575	1.76	1.82 ± 0.11
20.0	0.17	2.61	2.3	4260	1.31	1.37 ± 0.08
25.0	0.17	2.31	2.7	4755	1.22	1.16 ± 0.07
32.0	0.18	1.74	2.8	4080	1.07	1.04 ± 0.06
40.0	0.17	0.82	3.4	2730	0.81	0.77 ± 0.05

*$\Gamma = \frac{v_c}{A_r}(c_c - c_b)$.

†Γ_a is the average value of the surface concentration of ApoH obtained from three independent measurements.

TABLE 4 Parameters of the mixed monolayer of DPPG and ApoH at different surface pressure

Surface pressure π (mN/m)	Total area of mixed monolayer S (cm^2)[a]	Extended area after ApoH penetration A_{ex} (cm^2)	Average area per ApoH A_a (Å^2)[†]	Total number of ApoH N_t ($\times 10^{14}$)[‡]	Degree of condensation ϕ[§]
16.0	107.45	45.34	4923 ± 294	2.18	0.65 ± 0.05
20.0	84.07	26.71	6529 ± 392	1.29	0.75 ± 0.05
25.0	66.81	14.98	7761 ± 460	0.86	0.80 ± 0.05
32.0	54.20	0.71	8601 ± 516	0.63	0.94 ± 0.05
40.0	47.50	0.00	11579 ± 692	0.41	1.00 ± 0.05

*S and A_{ex} were measured from the π-A isotherms of Fig. 3.

†$A_a = \dfrac{M_w \times 10^{23}}{N_A} \times \dfrac{1}{\Gamma_a}$, where Γ_a is represented in Table 3, and N_A equals to 6.02×10^{23}.

‡$N_t = \dfrac{S}{A_a}$, where $M_w = 5.4 \times 10^4$ g/mol, which is the molecular weight of ApoH.

§ϕ was measured according to the fluorescence microscope images.

the DPPG monolayer at different surface pressures are listed in Table 4. Table 4 also shows that the DPPG monolayer becomes more condensed with increasing surface pressure.

DISCUSSION

The three-dimensional structure of ApoH at an almost atomic level has been reported by Bouma et al. (1999) and Schwarzenbacher et al. (1999), respectively. The crystal structure of ApoH reveals that the five-short-consensus repeat (SCR) domains form a fishhook-like shape (J-shape). The overall dimensions of the ApoH molecule are 132 × 72 × 20 Å, and domains 1–4 have similar dimensions of 38 × 17 × 20 Å. The linear distance from the N- to C-terminal end is 130 Å, and the distance along the curve of the molecule is ~190 Å. The fifth domain has a positively charged area of ~2000 Å^2, which is implicated to be essential for electrostatic binding. It also carries an exposed hydrophobic loop within the charged region, suggested to be essential for membrane insertion. Although the crystal structure of ApoH is clearly known, why ApoH can play quite different physiological functions in vivo is still unclear. Concerning the fact that the interaction of ApoH with the lipid membrane is a basic mechanism related to its physiological and pathogenic functions, the problems of ApoH orienting and docking at the membrane surface is of extreme significance.

Both the results of the π-A isotherm and the surface protein concentration measurements show that ApoH molecules begin to be extruded out from the mixed monolayers when the surface pressure reaches the inflection of the isotherms. The fluorescence microscope observation shows that the proteins will concentrate in the liquid phase region at low surface pressures and that they also occur in the condensed domain region as the pressure is sufficiently increased. The surface concentration determination also provides evidence that a considerable amount of ApoH remains at the monolayer surface even if the whole monolayer is nearly in a condensed phase. The next section discusses the spatial state of membrane-attached ApoH according to these facts.

Orientation of ApoH at the surface of neutral lipid layer

Table 2 shows that the numerical values of N_t are nearly constant as π increases from 9.8 to 18.0 mN/m, and they are decreased as $\pi > 18.0$ mN/m. This provides direct evidence that ApoH squeezed into the subphase as $\pi > 18.0$ mN/m. These results are consistent with those observed in Fig. 1 *B*, where the isotherm exhibits an inflection at $\pi = 18.0$ mN/m, suggesting the proteins are extruded out at this pressure. The fluorescence micrographs show that membrane-attached proteins prefer to stay in the liquid phase. Based upon these findings, it can be assumed that the membrane-attached proteins, concentrating in the liquid phase, reach their saturation when increasing pressure to 18.0 mN/m. The proteins will then be extruded out as the pressure continues to increase. Assuming that all membrane-attached ApoH distributes in the liquid phase at $\pi <$ 18.0 mN/m, it follows that $N_l \approx N_t$ in this surface pressure region. Here, N_l represents the number of ApoH in the liquid phase. Assuming also that the protein surface concentration reaches its saturation in the liquid phase at $\pi =$ 18.0 mN/m and retains the saturation as $\pi > 18.0$ mN/m, then, the average area per ApoH in the liquid phase, A_l, is obtained as ~1584 Å^2 according to $A_l = S \times (1 - \phi)/N_l$. The reported section area of the fishhook-like ApoH by x-ray crystal, is 72 × 20 = 1440 Å^2. Here, the obtained A_l coincides with the reported value as well. Therefore, it appears that ApoH adopts an upright orientation in the liquid phase.

When the surface pressure is increased to 30.0 mN/m, most ApoH molecules are extruded out from the DPPC monolayer. This is according to the fact that the isotherm of mixed monolayer closes to overlap the isotherm of pure DPPC monolayer at this pressure (Fig. 1 *B*). The total number of protein (N_t in Table 2) shows, however, that only

TABLE 5 Distribution of the extruded ApoH out of the DPPC mixed monolayer

Surface pressure π (mN/m)	Number of ApoH squeezed into bulk N_{out} ($\times 10^{14}$)*	Number of ApoH in liquid phase N_l ($\times 10^{14}$)†	Number of ApoH beneath condensed domains N_c ($\times 10^{14}$)‡	Apparent area occupied by adsorbed ApoH beneath condensed domain A_c (Å^2)§
18.0	0 (0%)	3.11 (100%)	0 (0%)	—
22.0	0.46 (15%)	1.90 (61%)	0.75 (24%)	6538
26.0	0.67 (22%)	1.29 (41%)	1.05 (27%)	4747
30.0	0.80 (26%)	0.36 (11%)	1.95 (63%)	2982

*$N_{out} = 3.11 \times 10^{14} - Nt$, assuming the initial number of membrane-attached ApoH is 3.11×10^{14}.
†$N_l = S(1 - \varphi)/A_l$, where $A_l = S(1 - \varphi)/Nt$ at 18.0 mN/m.
‡$N_c = Nt - N_l$.
§$A_c = \dfrac{S\phi}{N_c}$.

a small amount of proteins (~26%) are squeezed into the subphase, and most of them remain in the membrane-surface region. A possible explanation is that most of the extruded proteins do not go into the bulk. This explanation also provides an interpretation for the contrast between the dark discrete domain and the light continuous region becoming weaker at a pressure of 30.0 mN/m (Fig. 2 *D*). A part of the extruded ApoH laterally shifts to and beneath the condensed domains. Thus, the extruded ApoH can be divided into three parts: N_{out}, the number of ApoH squeezed into the subphase; N_l, the number of ApoH retained in the liquid phase; and N_c, the number of ApoH relocating beneath the condensed phase. The numerical values of N_{out}, N_l and N_c are shown in Table 5. Table 5 shows that at pressure 30.0 mN/m the percentage of ApoH in the liquid phase and in the solid phase are 11% and 63%, respectively. Only ~26% of proteins are squeezed into the subphase. Furthermore, from the average value of the area of ApoH at pressure 30.0 mN/m, i.e., $A_a \approx 2700$ Å^2, it can be inferred that the ApoH molecules retain upright orientation when laterally moving from the liquid to the condensed phase region. Here, a schematic diagram (Fig. 5 *A*) is used to illustrate the process of ApoH being extruded out from the DPPC monolayer.

Orientation of ApoH at the surface of acidic lipid layer

Table 4 represents the surface concentration of ApoH in the ApoH-DPPG mixed monolayer (subphase concentration of ApoH is 3 nM) under different surface pressures. It is shown that when surface pressure increases above 16.0 mN/m (corresponding to the inflection of dotted line in Fig. 3), the total number of proteins decreases and the surface density of ApoH decreases also. This phenomenon is different from that in the case of the DPPC monolayer. Assuming that the proteins are saturated in the liquid phase region as $\pi = 16.0$ mN/m and extruded out when $\pi > 16.0$ mN/m, the protein's area can be calculated in the liquid phase. Table 4 shows $\phi = 0.65$ and $N_t = 2.18 \times 10^{14}$ at $\pi = 16.0$ mN/m. Thus, the average area per ApoH in the liquid phase, A_l, is obtained as ~1725 Å^2 according to $A_l = S \times (1 - \phi)/N_l$ and $N_l = N_t$. This value is comparable with that of the section area (~1440 Å^2) of the fishhook-like structure of ApoH reported by the x-ray crystal results. Therefore, the membrane-attached ApoH may also be in an upright orientation in the liquid phase in the DPPG monolayer.

It is notable from Table 4 that the averaged area A_a per ApoH in the DPPG monolayer is much larger than the one in the DPPC monolayer. For example, $A_a = 8601$ Å^2 at $\pi = 32.0$ mN/m for ApoH in the DPPG monolayer whereas $A_a = 2763$ Å^2 at $\pi = 30.0$ mN/m for ApoH in the DPPC monolayer. Also, the average area A_a increases drastically for ApoH in the DPPG mixture (see Table 4 as $\pi > 16.0$ mN/m) whereas it changes little for ApoH in the DPPC mixture (see Table 2 as $\pi > 18.0$ mN/m). It seems unreasonable that ApoH should adopt a similar state of orientation in the two types of monolayer. Using similar calculations to those used in Table 5, the numerical values of N_{out}, N_l, and N_c for the ApoH-DPPG mixed monolayer can be also obtained. The results are shown in Table 6. Table 6 shows that the apparent area occupied per ApoH at the

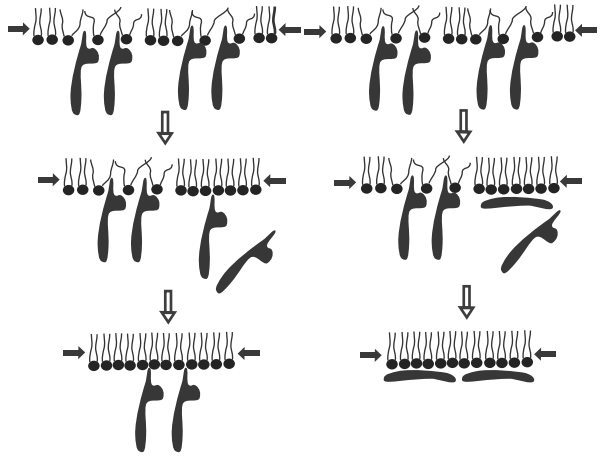

FIGURE 5 Schematic illustration of the process of ApoH squeezed out of the lipid monolayer by compression. (*A* and *B*) Orientation and lateral distribution of ApoH at the surface of the DPPC and the DPPG monolayer, respectively.

TABLE 6 Distribution of the extruded ApoH out of the DPPG mixed monolayer

Surface pressure π (mN/m)	Number of ApoH squeezed into bulk N_{out} ($\times 10^{14}$)*	Number of ApoH in liquid phase N_l ($\times 10^{14}$)†	Number of ApoH beneath condensed domains N_c ($\times 10^{14}$)‡	Apparent area occupied by adsorbed ApoH beneath condensed domain A_c (Å^2)§
16.0	0 (0%)	2.18 (100%)	0 (0%)	
20.0	0.89 (41%)	1.22 (56%)	0.07 (3%)	92971
25.0	1.32 (61%)	0.78 (36%)	0.09 (4%)	62633
32.0	1.55 (71%)	0.19 (9%)	0.44 (20%)	11542
40.0	1.77 (81%)	0 (0%)	0.41 (19%)	11579

*$N_{out} = 2.18 \times 10^{14} - Nt$, assuming the initial number of membrane-attached ApoH is 2.18×10^{14}.
†$N_l = S(1 - \varphi)/A_l$, where $A_l = S(1 - \varphi)/Nt$ at 16.0 mN/m.
‡$N_c = Nt - N_l$.
§$A_c = \dfrac{S\phi}{N_c}$.

surface of the condensed domain, A_c, has a similar value, ~11,550 Å^2 in the pressure region from 32.0 to 40.0 mN/m. Furthermore, the numbers of ApoH under the condensed domain begin to decrease in this surface pressure range. These results suggest that the proteins beneath the condensed domains come close to saturation when the pressure is above 32.0 mN/m. In a separated experiment (Sun et al., 2000), the surface pressure of the pure ApoH monolayer began to rise when the average molecular area was compressed to ~10,000 Å^2, indicating that the proteins began to touch each other at the interface. This value is identical to that of A_c in the current work, i.e., $\pi > 32.0$ mN/m; therefore, $A_c \approx 11{,}550$ can be considered to be a molecular arrangement that is close to saturation. The reported crystal structure shows that the lateral area of the J-shaped ApoH is $132 \times 72 = 9504$ Å^2, which is compatible with the obtained A_c. Thus, the results of the current work suggest that ApoH may lie on the surface of the condensed domains of the DPPG monolayer with a flat orientation.

The protein-extruding process in the ApoH-DPPG mixed monolayer can be assumed. In the lower-surface-pressure region ($\pi < 16.0$ mN/m), membrane-attached ApoH concentrates in the liquid phase with an upright orientation. As surface pressure increases to 16.0 mN/m the ApoH molecules reach their saturation in the liquid phase. The ApoH then begins to be extruded out from the monolayer as π over the point 16.0 mN/m. The membrane-attached ApoH will now have three different ways to go: N_l, N_{out}, and N_c as shown in Table 6. Unlike the case of the ApoH-DPPC mixed monolayer, here, a part of the membrane-attached ApoH will change its orientation from the upright to the flat state as it shifts from the liquid to the condensed phase region. This process of ApoH being extruded out from the DPPG monolayer is illustrated in schematic diagram Fig. 5 *B*.

Thus, ApoH can have two forms of orientation on the surface of the acidic lipid monolayer. These two forms of orientation are dependent upon the phase status of the monolayer on which ApoH binds. Previous work (Wang et al., 1999) reported that two types of spatial orientation of ApoH exist when reacting with anionic phospholipid vesicles. The present results give this model further support. Since phase separation exists in biological membranes, the two forms of orientation of ApoH in the acidic lipid-containing membrane may be related to the variety of physiological and pathogenic functions of the protein.

Determining section area of the inserted domain

The extended area A_{ex} after ApoH penetration can be measured with π-A isotherms. Assuming that A_{ex} is the only result of protein penetration, the cross-section area of insertion domain of ApoH can be calculated by dividing A_{ex} with the number of ApoH molecules in the liquid-expanded phase of the lipid monolayer. This calculation becomes complicated due to the influence of ApoH penetration on monolayer crystallization (Heckl et al., 1987). As seen from Tables 2 and 4, the degree of condensation of the mixed monolayer ϕ is ~1 at a surface pressure of 30.0 mN/m. This means that all lipid molecules exhibit substantial vertical orientation, and ApoH insertion has little influence on the area occupied by the lipid. Under such conditions, the area occupied by the insertion domain per ApoH, A_{in}, according to $A_{in} = A_{ex}/N_l$, and $N_l = S(1 - \phi)/A_l$, can be calculated, as shown in the following formula:

$$A_{in} = \frac{A_l}{1 - \phi} \times \frac{A_{ex}}{S} \tag{4}$$

The calculated A_{in} shows different values for the DPPC and the DPPG lipid layer. In the case of the membrane-attached ApoH in the DPPC monolayer, A_{in} is ~244 Å^2 (30.0 mN/m) whereas in the DPPG monolayer it is ~374 Å^2 (32.0 mN/m).

The above two average A_{in} values reveal that only a small part of the membrane-attached ApoH inserts into the mixed monolayer. This result is consistent with the results reported for the x-ray crystal structure. Their data suggested that only a small loop of the fifth domain (311–317 loop) plays a crucial role in the insertion. The discrepancy between the

two values may be due to the electrostatic interaction, because the loop is besieged in the positively charged area of the fifth domain. The electrostatic force may enhance the membrane insertion so that A_{in} in the DPPG monolayer is larger.

This work was supported by the National Natural Science Foundation of China.

REFERENCES

Aoubala, M., M. Ivanova, I. Douchet, A. D. Caro, and R. Verger. 1995. Interfacial binding of human gastric lipase to lipid monolayers, measured with an ELISA. *Biochemistry.* 34:10786–10793.

Blank, M., D. Faden, A. Tincani, J. Kopolovic, I. Goldberg, B. Gilburd, F. Allegri, G. Balestrieri, G. Valesini, and Y. Shoenfeld. 1994. Immunization with anticardiolipin cofactor (β_2-glycoprotein I) induces experimental antiphospholipid syndrome in naive mice. *J. Autoimmun.* 7:441–455.

Bouma, B., P. G. de Groot, J. M. H. van den Elsen, R. B. G. Ravelli, A. Schouten, M. J. Simmelink, R. H. Derksen, J. Kroon, and P. Gros. 1999. Adhesion mechanism of human β_2-glycoprotein I to phospholipids based on its crystal structure. *EMBO. J.* 18:5166–5174.

Brighton, T. A., B. J. Hogg, Y. P. Dai, B. H. Murray, B. H. Chong, and C. N. Chesterman. 1996. β_2-glycoprotein I in thrombosis: evidence for a role as a natural anticoagulant. *Br. J. Haematol.* 93:185–194.

Gargouri, Y., H. Moreau, G. Pieroni, and R. Verger. 1989. Role of a sulfhydryl group in gastric lipases: a binding study using the monomolecular-film technique. *Biochemistry.* 180:367–373.

Gargouri, Y., G. Pieroni, C. Riviere, C. Sarda, and R. Verger. 1986. Inhibition of lipases by proteins: a binding study using dicaprin monolayers. *Biochemistry.* 25:1733–1738.

Hagihara, Y., K. Enjyoji, Y. Omasa, Y. Katakura, K. Suga, M. Igarashi, E. Matsura, H. Kato, T. Yoshimura, and Y. Goto 1997. Structure and function of the recombinant fifth domain of human β_2-glycoprotein I: effects of specific cleavage between Lys77 and Thr78. *J. Biochem.* 121:128–137.

Hagihara, Y., Y. Goto, H. Kato, and T. Yoshimura. 1995. Role of the N- and C-terminal domains of bovine β_2-glycoprotein I in its interaction with cardiolipin. *J. Biochem.* 118:129–136.

Heckl, W. M., B. N. Zaba, and H. Mohwald. 1987. Interactions of cytochromes b5 and c with phospholipid monolayers. *Biochim. Biophys. Acta.* 903:166–176.

Hunt, J., and S. Krilis. 1994. The fifth domain of β_2-glycoprotein I contains a phospholipid binding site (Cys281-Cys288) and a region recognized by anticardiolipin antibodies. *J. Immunol.* 152:653–659.

Ichinose, A., R. E. Botttenus, and E. W. Davie. 1990. Characterization of the gene for human plasminogen, a key proenzyme in the fibrinolytic system. *J. Biol. Chem.* 265:13411–13414.

Kertesz, Z., B. B. Yu, A. Steinkasserer, H. Haupt, A. Benham, and R. B. Sim. 1995. Characterization of binding of human β_2-glycoprotein I to cardiolipin. *Biochem. J.* 310:315–321.

Liu, Z., H. Qin, C. Xiao, C. H. Wen, S. P. Wang, and S. F. Sui. 1995. Specific binding of avidin to biotin containing lipid lamella surfaces studied with monolayers and liposomes. *Eur. Biophys. J.* 24:31–38.

Mehdi, H., A. Naqvi, and M. I. Kamboh. 2000. A hydrophobic sequence at position 313–316 (Leu-Ala-Phe-Trp) in the fifth domain of apolipoprotein H (β_2-glycoprotein I) is crucial for cardiolipin binding. *Eur. J. Biochem.* 267:1770–1776.

Mi, L. Z., H. W. Wang, and S. F. Sui. 1997. Interaction of rabbit C-reactive protein with phospholipid monolayers studied by micro-fluorescence film balance with an externally applied electric field. *Biophys. J.* 73: 446–451.

Möhwald, H. 1990. Phospholipid and phospholipid-protein monolayers at the air/water interface. *Annu. Rev. Phys. Chem.* 41: 441–476.

Momsen, W. E., and H. L. Brockman. 1997. Recovery of monomolecular films in studies of lipolysis. *Methods Enzymol.* 286:292–305.

Rietsch, J., F. Pattus, P. Desnuelle, and R. Verger. 1977. Further studies of mode of action of lipolytic enzymes. *J. Biol. Chem.* 252:4313–4318.

Schousboe, I. 1979. Purification, characterization, and identification of an agglutinin in human serum. *Biochim. Biophys. Acta* 579:396–408.

Schultze, H. E., K. Heide, and H. Hampt. 1961. Über ein bisher unbekanntes niedermolekulares β2-Globulin des Humanserums. *Naturwissenschaften.* 23:719–724.

Schwarzenbacher, R., K. Zeth, K. Diederichs, A. Gries, G. M. Kostner, P. Laggner, and R. Prassl. 1999. Crystal structure of human β_2-glycoprotein I: implications for phospholipid binding and the antiphospholipid syndrome. *EMBO. J.* 18:6228–6239.

Shiozaka, A., K. Niiya, F. Higuchi, S. Tashiro, T. Arai, R. Izumi, and N. Sakuragawa. 1994. Ellagic acid/phospholipid-induced coagulation and dextran sulfate-induced fibrinolytic activities in β_2-glycoprotein I-depleted plasma. *Thromb. Res.* 76:199–210.

Sun, Y. T., S. X. Wang, and S. F. Sui. 2000. Penetration of human apolipoprotein H into air/water interface with and without phospholipid monolayers. *Colloid Surf. A.* 175:105–112.

Wang, S. X., G. P. Cai, and S. F. Sui. 1998. The insertion of human apolipoprotein H into phospholipid membranes: a monolayer study, *Biochem. J.* 335:225–232.

Wang, S. X., G. P. Cai, and S. F. Sui. 1999. Intrinsic fluorescence study of the interaction of human apolipoprotein H with phospholipid vesicles. *Biochemistry.* 38:9477–9484.

Wang, S. X., Y. T. Sun, and S. F. Sui. 2000. Membrane-induced conformational change in human apolipoprotein H. *Biochem. J.* 348:103–106.

Willems, G. M., M. P. Janssen, M. M. A. Pelsers, P. Galli, M. Comfurius, R. F. A. Zwaal, and E. M. Bevers. 1996. Role of divalency in the high-affinity binding of anticardiolipin antibody-β_2-glycoprotein I complexes to lipid membranes. *Biochemistry.* 35:13833–13842.

Wurm, H. 1984. β_2-glycoprotein I (apolipoprotein H) interactions with phospholipid vesicles. *Int. J. Biochem.* 16:511–515.